

## Article

# Droplet Based Estimation of Viscosity of Water–PVP Solutions Using Convolutional Neural Networks

Mohamed Azouz Mrad <sup>1,\*</sup>, Kristof Csorba <sup>1</sup>, Dorián László Galata <sup>2</sup>, Zsombor Kristóf Nagy <sup>2</sup>  
and Hassan Charaf <sup>1</sup>

<sup>1</sup> Department of Automation and Applied Informatics, Faculty of Electrical Engineering and Informatics, Budapest University of Technology and Economics, Műgyetem rkp.3., H-1111 Budapest, Hungary; csorba.kristof@vik.bme.hu (K.C.); charaf.hassan@aut.bme.hu (H.C.)

<sup>2</sup> Department of Organic Chemistry and Technology, Faculty of Chemical Technology and Biotechnology, Budapest University of Technology and Economics, Budafoki út 8., F. II., H-1111 Budapest, Hungary

\* Correspondence: mmrad@edu.bme.hu

**Abstract:** The viscosity of a liquid is the property that measures the liquid's internal resistance to flow. Monitoring viscosity is a vital component of quality control in several industrial fields, including chemical, pharmaceutical, food, and energy-related industries. In many industries, the most commonly used instrument for measuring viscosity is capillary viscometers, but their cost and complexity pose challenges for these industries where accurate and real-time viscosity information is vital. In this work, we prepared fourteen solutions with different water and PVP (Polyvinylpyrrolidone) ratios, measured their different viscosity values, and produced videos of their droplets. We extracted the images of the fully developed droplets from the videos and we used the images to train a convolutional neural network model to estimate the viscosity values of the water–PVP solutions. The proposed model was able to accurately estimate the viscosity values of samples of unseen chemical formulations with the same composition with a low MSE score of 0.0243 and R2 score of 0.9576. The proposed method has potential applications in scenarios where real-time monitoring of liquid viscosity is required.

**Keywords:** viscosity; convolutional neural networks; water–PVP; Polyvinylpyrrolidone; viscosity estimation



**Citation:** Mrad, M.A.; Csorba, K.; Galata, D.L.; Nagy, Z.K.; Charaf, H. Droplet Based Estimation of Viscosity of Water–PVP Solutions Using Convolutional Neural Networks. *Processes* **2023**, *11*, 1917. <https://doi.org/10.3390/pr11071917>

Academic Editor: Udo Fritsching

Received: 6 May 2023

Revised: 9 June 2023

Accepted: 22 June 2023

Published: 26 June 2023



**Copyright:** © 2023 by the authors. Licensee MDPI, Basel, Switzerland. This article is an open access article distributed under the terms and conditions of the Creative Commons Attribution (CC BY) license (<https://creativecommons.org/licenses/by/4.0/>).

## 1. Introduction

The internal resistance of a liquid to flow or shear is measured by its viscosity. This fundamental characteristic parameter is essential for quality control in various industrial areas, including but not limited to the pharmaceutical, food, chemical, and energy-related sectors [1]. In the pharmaceutical industry, viscosity plays a significant role in ocular drug absorption and Indomethacin dissolution [2], as well as in determining nanoparticle sizes, drug contents, and dissolution profiles [3]. In the food industry, viscosity is an important quality parameter, which affects the texture, consistency, appearance, and taste of the product [4]. Measuring the viscosity accurately is crucial in the design of industrial equipment and chemical processes. This is particularly important for applications that involve molten salts [5] and in simulating reservoirs, forecasting production, and planning thermal enhanced oil recovery methods to improve recovery [6,7]. Various instruments are available to measure viscosity, including capillary viscometers, orifice viscometers, rotational viscometers, and vibrational and ultrasonic viscometers. The capillary viscometer is the most commonly used method in several industries due to its affordability and ease of use. This method involves measuring the time taken for a specific volume of liquid to flow through a narrow tube under a given pressure [8]. Viscosity measurements through these invasive methods require laboratory conditions with constant temperature control, resulting in high costs, and they also affect the accuracy of the measurements. For example,

the accuracy of heavy oil viscosity measurements can be affected by sample handling, storage, and cleaning procedures and by the selection of viscometers and the experimental procedures followed by different operators [9]. This makes these methods unsuitable for continuous in-process monitoring and intervention in case of errors. Thus, it is crucial to develop a cost-effective, time-efficient, and accurate alternative for viscosity measurement.

Employing machine learning and image processing algorithms to estimate viscosity values is a potential alternative to the conventional viscosity measurement techniques. Using image processing and supervised learning techniques, Caponi et al. were able to predict the viscosity of hydrocarbons located at a particular reservoir depth in a heavy oil reservoir situated in California [10]. Zhang et al. created machine learning models that can process biomass compositions analysis and pyrolysis conditions to predict the yield, viscosity, and oxygen–carbon ratio (O/C) of bio-oil [11]. Cengiz et al. used Extreme Learning Machine (ELM), Multi-Layer Perceptron (MLP), and K Nearest Neighbor (KNN) methods to predict the kinematic viscosity of fuel oil [12]. Rahmanifard et al. trained 38 supervised machine learning algorithms to predict gas component viscosity using data of independent variables that impact the viscosity of pure gas components [13].

Researchers have employed artificial neural networks to estimate the dynamic viscosity of various substances. Afrand et al. predicted the dynamic viscosity of a hybrid nanolubricant using an optimal ANN model [14]. Esfe et al. demonstrated the high accuracy of their model in predicting the dynamic viscosity of ferromagnetic nanofluids [15]. Additionally, Al-Amoudi et al. proposed artificial neural network models to predict the viscosity of undersaturated, saturated, and dead oil in Yemeni fields, utilizing laboratory measurements of oil samples [16]. Furthermore, Nigerian crude oil viscosity has been predicted using 32 datasets that include reservoir temperature, oil and gas gravity, and the solution gas–oil ratio, through the use of artificial neural networks [17].

The correlation between liquid droplets and liquid viscosity has been the subject of several research studies.

In their paper [18], H. Zhu et al. revealed the correlation between extensional viscosity and spray droplet sizes of polymer spray solutions. According to Wang et al.'s study in [19], an increase in liquid viscosity results in a logarithmic increase in droplet diameter in vertical gas–liquid annular flows. The increase is initially rapid but slows down as the viscosity increases. The impact of viscosity on droplet–droplet collision outcomes was investigated by Gotaas et al. in their research reported in [20].

Some researchers have investigated the application of image processing techniques for the measurement of liquid viscosity. In their study published in [21], Kheloufi et al. utilized video analysis of falling ball viscometers to measure the fall height of a ball and compute the viscosity of the fluid under study. Mrad et al. employed an artificial neural network model to accurately classify droplets of water–PVP solutions into different viscosity categories [22]. Santhosh and Shenoy used a combination of imaging and artificial neural network techniques to accurately estimate the viscosity of a liquid. Specifically, they captured refracted laser images using a camera; processed them using thresholding, filtering, and histogram techniques; and used an artificial neural network to establish the relationship between the processed data and the viscosity. The results of their study were published in [23].

The convolutional neural network (CNN) is a well-known deep learning architecture inspired by the natural visual perception mechanism of the living creatures. CNNs have a wide range of applications, such as text recognition, speech, and natural language processing. However, they are mostly employed in image recognition systems [24]. CNNs were applied in image classification in various industries. Iwata et al. applied a CNN to classify scanning electron microscopy (SEM) images of pharmaceutical raw material powders to determine if a CNN can evaluate particle morphology [25]. Ghorbani et al. trained a convolutional neural network with a visual dataset of oil spills containing images from different altitudes and geographical locations to detect the existence of an oil spill in an image with an accuracy of 92% [26]. CNNs were also used for viscosity estimation: Vasconcelos et al. created a CNN model that estimated the elasticity and

viscosity parameters from simulated shear wave motion images [27]. Mohan et al. used CNN to extract key features from a video of fluid flow and fed it to a recurrent neural network (RNN) to estimate the viscosity of the fluid [28].

Due to the advantages of the ability of convolutional neural networks to automatically learn and extract relevant features from images along with the features and information that an image of a liquid droplet can provide, they appear to be a promising non-invasive continuous method to estimate the viscosity value of the corresponding droplet.

In this study, we prepared fourteen solutions with different water and PVP (Polyvinylpyrrolidone, which is a water-soluble polymer) ratios and measured their viscosity values using a viscometer. We carefully recorded videos of the droplets of these solutions as they dropped from a syringe pump using a high-quality monochrome camera, thereby capturing their exact behavior and characteristics. Using the data we generated, we aimed to train a convolutional neural network model that would be capable of accurately estimating the viscosity value of the given solution based on its droplets' images.

## 2. Materials and Methods

### 2.1. Materials

We used Povidone (PVPK30), which was provided to us by BASF (Ludwigshafen, Germany). The procedure for preparing the PVP solution involved dissolving 20 g of PVP in 100 mL of distilled water that had a  $20 \mu\text{S}/\text{cm}$  resistance. PVP solutions were used because PVP is a polymer that is soluble in water and the concentration of PVP in the solution is known to influence the viscosity. Therefore, PVP is ideal for preparing solutions with different viscosities. However, the flow behavior will not be investigated in this study as it has been investigated in the literature. MINESHITA and al. observed that non-Newtonian flow behavior was observed in all ranges of shear stress for Polyvinylpyrrolidone solutions [29].

### 2.2. Measurement Setup

The Department of Organic Chemistry and Technology at the Faculty of Chemical Technology and Biotechnology, Budapest University of Technology and Economics, provided us with the necessary materials and software for conducting the experiment. These included fourteen 500 mL laboratory bottles, a one-channel syringe pump SEP-10S PLUS, a transparent rubber tube, a laboratory dropper, an LED white light panel, and one lab beaker. The department also provided us with the recording materials: an acA720-520um USB 3.0 monochrome camera manufactured by Basler AG, a German company founded in 1988 that specializes in the design and production of digital cameras, Pylon Viewer, and PharmaVision Videometry software.

### 2.3. Methods

#### 2.3.1. Experimental Setup

For the experiment, a total of fourteen solution samples (formulations) were created by combining the PVP solution and distilled water in various ratios, resulting in solutions with a range of viscosity values, as outlined in Table 1. The objective of the experiment was to capture the formation process of droplets from each of these solutions via video recording.

During the experiment, the liquid sample was dispensed from an automatic syringe pump through a transparent rubber tube to a pipette dropper at a controlled rate of 20 mL per hour. The dropper was held in a fixed perpendicular position to the horizontal plane using a stand while a lab beaker was placed directly beneath it to collect the falling droplets. A high-quality monochrome camera, held in place using another stand, was positioned behind the dropper to capture videos of the droplet formation process. To ensure a uniform background, a strong white LED panel was positioned behind the dropper. The videos were recorded from the moment a droplet appeared in the dropper until it fell into the beaker using a frame rate of 200 frames per second and dimensions of 600 by 1000 pixels. The recorded videos were in black and white and were analyzed using the internally developed software, PharmaVision Videometry. The experiment was performed for each

of the fourteen solution samples, with key parameters, such as the dropper and camera positions and infusion rate, kept constant. To ensure the accuracy and comparability of the results, the syringe and rubber tube were thoroughly cleaned before each sample preparation to eliminate any residue that could affect subsequent measurements. A total of fourteen videos were recorded, each with a duration of 10 min, providing informative data on the characteristics of droplets during their formation stages. The experimental setup and test can be viewed in Figures 1 and 2.

**Table 1.** Different chemical formulations used in sample preparation. Formulations chosen for testing are displayed in bold.

Formulation Name (PVP%)	Distilled Water (mL)	PVP Solution (mL)
PVP00.0	75	0
PVP05.0	71.25	3.75
<b>PVP07.5</b>	<b>69.375</b>	<b>5.625</b>
PVP10.0	67.5	7.5
PVP15.0	63.75	11.25
PVP20.0	60	15
PVP25.0	56.25	18.75
<b>PVP27.5</b>	<b>54.375</b>	<b>20.625</b>
PVP30.0	52.5	22.5
PVP35.0	48.75	26.25
PVP40.0	45	30
<b>PVP42.5</b>	<b>43.125</b>	<b>31.825</b>
PVP45.0	41.25	33.75
PVP50.0	37.5	37.5

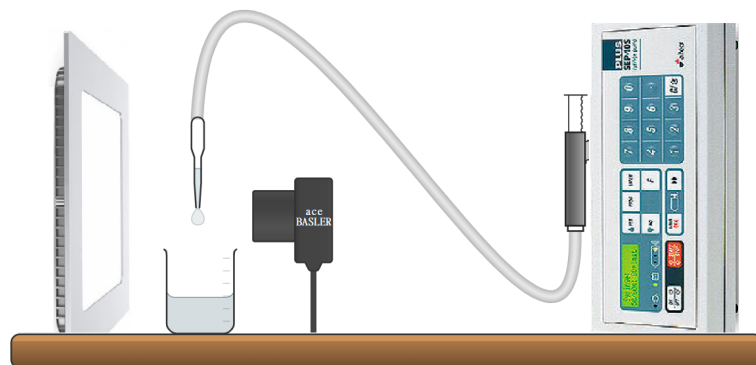


**Figure 1.** Experimental setup.

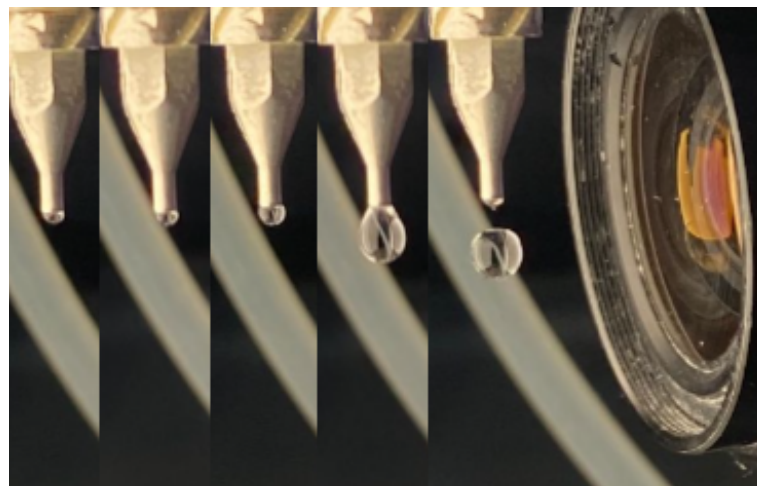


**Figure 2.** Experimental setup in test: droplet in different states.

### 2.3.2. Viscosity Measurement

The viscosity values of the various samples were quantified using the DMA 4500 M viscometer manufactured by Anton Paar, an Austrian company founded in 1922, and were documented in Table 2. The measurements were obtained by determining the rolling time of a 1.5 mm diameter steel ball through the sample in a capillary tube angled at  $-45^\circ$  while the temperature of the sample was maintained at a constant  $25.00^\circ\text{C}$ . The values are in mPa·s (millipascal-second), which is a unit of dynamic viscosity. It is equal to one-thousandth of a pascal-second (Pa·s) that is the SI unit of dynamic viscosity. The values presented are the apparent viscosity values given by the instrument.

**Table 2.** Viscosity values of water–PVP samples. Samples chosen for testing are displayed in bold.

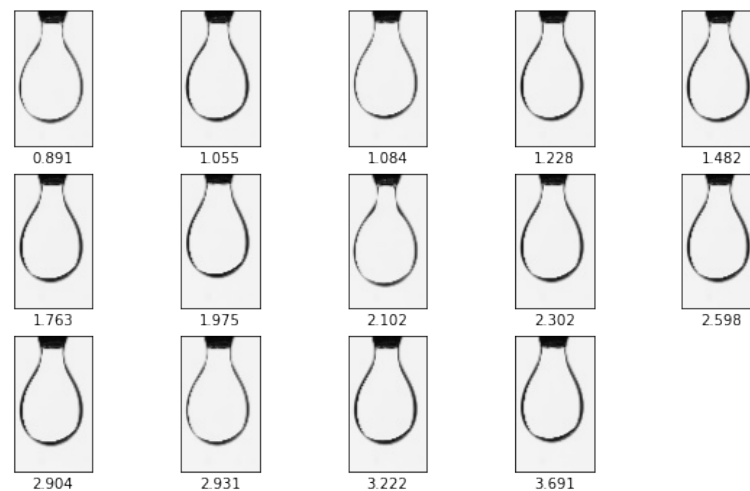
Formulation Name (PVP%)	Viscosity in mPa·S
PVP00.0	0.891
PVP05.0	1.055
<b>PVP07.5</b>	<b>1.084</b>
PVP10.0	1.228
PVP15.0	1.482
PVP20.0	1.763
PVP25.0	1.975
<b>PVP27.5</b>	<b>2.102</b>
PVP30.0	2.302
PVP35.0	2.598
PVP40.0	2.904
<b>PVP42.5</b>	<b>2.931</b>
PVP45.0	3.222
PVP50.0	3.691

### 2.3.3. Data Analysis

In this study, we processed and analyzed the videos of the droplets to identify valuable information. Various features of the droplets were identified, such as the duration of the droplet formation process; the area, perimeter, and diameter of the droplet; and the maximum length and width the droplet can reach before it falls. In the videos, the droplet can be seen in three different states, as shown in Figure 3. However, we focused on capturing images of the droplets just before detachment from the dropper as it provides more information about the droplets to be used for comparison with other droplets in a similar state. We extracted 6074 images of droplets in the “before-detachment” state. We carefully examined each image and made adjustments when necessary so that any differences between the images only reflected changes in the droplet characteristics. The captured images were adjusted to a resolution of 53 by 91 pixels, as shown in Figure 4, using OpenCV, a publicly available library of functions that comprises a range of image processing techniques, including but not limited to image filtering and transformation, object tracking, and feature detection [30]. This was to ensure that the input size of the CNN is consistent across all images and to address the issue of large file sizes and memory usage. The pixel values of the images were normalized to a range between 0 and 1 to improve the convergence rate during the training of the proposed model by dividing the pixel values by 255. The resulting dataset is represented in Table 3.

**Table 3.** Number of captured images for each formulation.

Formulation Name (PVP%)	Number of Images
Training and validation set	
PVP00.0	437
PVP05.0	450
PVP10.0	473
PVP15.0	447
PVP20.0	394
PVP25.0	440
PVP30.0	393
PVP35.0	442
PVP40.0	440
PVP45.0	435
PVP50.0	437
Testing set	
PVP07.5	425
PVP27.5	422
PVP42.5	439
Total	6074

**Figure 3.** Stages of droplet formation, including three droplets: a droplet in the development phase on the left, a completely formed droplet just before detachment in the middle, and a detached droplet on the right.**Figure 4.** Resized images of droplets with their corresponding viscosity values.

### 2.3.4. Convolutional Neural Networks

CNNs typically consist of multiple layers, including convolutional, pooling, activation, and fully connected layers, each playing a unique role in the processing and analysis of the input image. The convolutional layers apply a set of filters to the input image to extract relevant features, while the pooling layers reduce the output of the convolutional layers, reducing the dimensionality of the data. The fully connected layers use the extracted features to make predictions or classifications. The output layer produces the final prediction or classification result. By combining these layers in a specific architecture, CNNs can achieve state-of-the-art performance on various image processing tasks, including object detection, recognition, and segmentation [31]. In this study, our goal was to estimate the viscosity values of the solution sample using the images of the droplets.

For this objective, convolutional neural network (CNN) models were created utilizing the Keras library, a high-level open-source Python library for deep learning that is designed to run on top of TensorFlow [32]. The activation function ReLU was utilized by the models on the different layers. The weights on the models were optimized using the Adam optimizer and the mean squared error (MSE) was the loss function used on the proposed models. The dataset consists of 6074 images from which 3830 images were used for training and 958 images were used for validation (20% of the training set). The samples chosen for validation were selected uniformly from the training data. For testing, we used data from three distinct chemical formulations (PVP07.5, PVP27.5, and PVP42.5) that were not included in the training or validation data of the models. The data used for testing consists of 1286 images, which is around 33% of the data used for training the models.

### 2.3.5. Evaluation Measurement

To provide a comprehensive evaluation of the proposed models' performance in the estimation of the viscosity of water–PVP solutions, we decided to check the following evaluation metrics, which are commonly used for similar regression problems:

- **Mean squared error (MSE):** The MSE calculates the average of the squared differences between the predicted and actual values. It is the metric used by the proposed models for the loss function.

$$1/n \sum_{i=1}^n (y_{pred}^i - y_{true}^i)^2 \quad (1)$$

where  $n$  is the number of samples in the dataset, and  $y_{pred}^i$  and  $y_{true}^i$  represent the predicted and actual values for the  $i$ th sample, respectively.

- **Mean absolute error (MAE):** This metric calculates the average absolute difference between the predicted and actual values. The MAE is a good metric to use when the dataset has a large number of outliers because it is less sensitive to outliers than other metrics such as MSE. Since our data consist of images that are quite similar to the naked eye but might hide some outliers, it would be important to check the MAE.

$$1/n \sum_{i=1}^n |y_{pred}^i - y_{true}^i| \quad (2)$$

where  $n$  is the number of samples in the dataset, and  $y_{pred}^i$  and  $y_{true}^i$  represent the predicted and actual values for the  $i$ th sample, respectively.

- **R2 score (coefficient of determination):** The  $R^2$  is a metric that measures the proportion of the variance in the dependent variable that is predictable from the independent variables. It provides an indication of how well the model fits the data. The  $R^2$  score ranges from 0 to 1, with 1 indicating a perfect fit.

$$\frac{MSE}{Var(y_{true}^i)} \quad (3)$$

where  $Var(y_{true}^i)$  is the variance of the actual values.

Together, these metrics provide a good overall evaluation of the performance of the CNN models in estimating the viscosity values of water–PVP solutions. By evaluating the MAE, MSE, and R2, we can assess the accuracy of the models. This information can be used to compare different models and choose the best one for our task.

### 3. Results and Discussion

Multiple CNN models were created, and various hyperparameters were tuned to find the best-performing model. Specifically, the following parameters were varied during the models' creation: the number of convolutional layers, the number of filters in each convolutional layer, the size of the convolutional filters, the pooling method and size, the number and size of the fully connected layers, and the learning rate of the optimizer. Three models were selected to be presented, each with a different architecture that determines how it processes the input images and makes predictions:

- **SimpleModel:** The SimpleModel has a basic architecture, which consists of 1 convolutional layer with 32 filters of size (3, 3), followed by a max-pooling layer of size (2, 2), a flatten layer, 2 dense layers of sizes 64 and 1, respectively, and a dropout layer with a rate of 0.5. The input shape of the SimpleModel is (91, 53, 3), which represents the size of the input droplet images.
- **DeepModel.** This model architecture is more complex than the SimpleModel, consisting of two convolutional layers with 32 and 64 filters of sizes (5, 5) and (5, 5), respectively, followed by 2 max-pooling layers of size (2,2), a flatten layer, 2 dense layers of sizes 128 and 1, respectively, and a dropout layer with a rate of 0.5. The input shape of the DeepModel is also (91, 53, 3).
- **ComplexModel.** This model architecture is the most complex of the 3 models and includes 3 convolutional layers with 32, 64, and 64 filters of sizes (7, 7), (7, 7), and (7, 7), respectively, followed by 3 max-pooling layers of size (2, 2), a flatten layer, 3 dense layers of sizes 128, 64, and 1, respectively, and 2 dropout layers with a rate of 0.5. The input shape of the ComplexModel is also (91, 53, 3).

In all three models, the first layer is a convolutional layer that applies filters to the input droplet images, extracting features such as edges and patterns. The max-pooling layer then reduces the spatial size of the feature maps, reducing the number of parameters in the model to prevent overfitting. The flatten layer reshapes the output of the convolutional layer into a 1D array, which is then passed to the dense layers that perform the regression task. The dropout layer is used to randomly drop some of the neurons during training, preventing overfitting and improving the generalization performance of the model. The different architectures are shown in Figure 5.

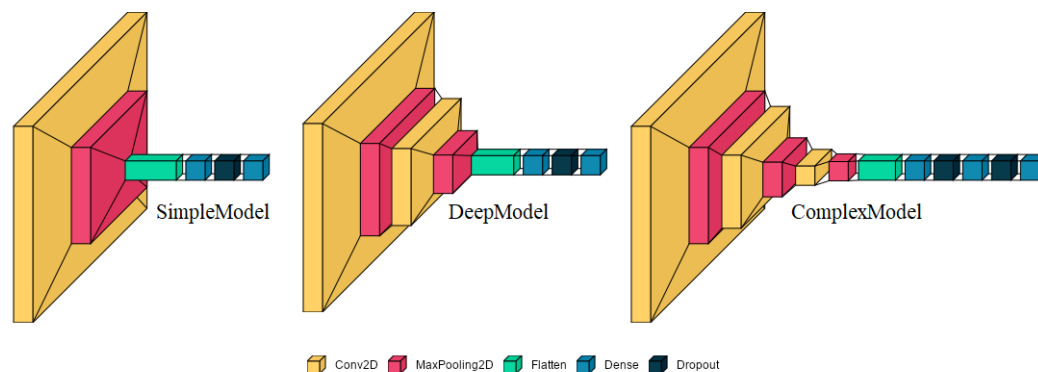


**Figure 5.** CNN models' architectures.

The models were trained on 100 epochs, with an early stopping introduced to monitor the validity loss with a patience of 15 epochs. The training and loss curves are presented

in Figure 6. We can notice that the curve for the SimpleModel decreases slowly initially but then stops improving at the later epochs. For the DeepModel, the curve decreases rapidly over the initial epochs as the model begins to learn the patterns in the data, and it continues to decrease at a slower rate during the remaining training epochs. The validation curve generally follows a similar trend to the training loss curve with some very small fluctuations. The ComplexModel curve is similar to the Deepmodel curve with a slower learning rate and with higher fluctuations on the validation curve.

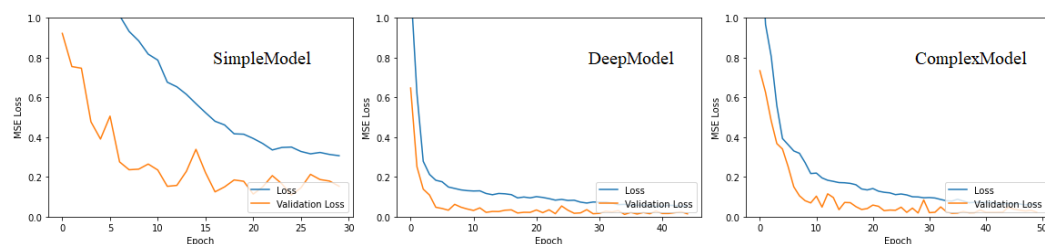


**Figure 6.** CNN models' loss curves.

The performance of each model was evaluated using the metrics presented in Section 2.3.5. The results are presented in Table 4. The first model, the SimpleModel, did not perform well, with an MSE score of 0.1798 and R2 score 0.6867 on the testing set. This suggests that the architecture was not complex enough to accurately capture the features and patterns in the droplet images that are relevant to predicting viscosity. The second model, the DeepModel, performed significantly better than the SimpleModel, with an MSE score of 0.0243 and R2 score of 0.9576 on the dataset. The architecture of the DeepModel, with its additional convolutional and max-pooling layers, was able to extract more relevant features from the droplet images and significantly improve the accuracy of the viscosity predictions. The third model, the ComplexModel, also performed reasonably well with an MSE score of 0.0400 and R2 score 0.9302 on the testing set, but not as well as the DeepModel. This indicates that adding more convolutional and max-pooling layers beyond a certain point does not necessarily improve the performance of the model and may lead to overfitting. These results demonstrate the importance of the architecture of CNN models for accurately estimating viscosity from droplet images. The DeepModel architecture was found to be the most effective for this task, suggesting that for a similar task a moderate level of complexity is optimal for capturing the relevant features in the images.

The DeepModel results indicate that the model is both robust and capable of generalization, as it was able to accurately estimate the viscosity values of new, unseen images that were not used during training. Most importantly, the model was able to predict the viscosity of the testing set images of water–PVP formulations that it had not been previously exposed to or trained on. The viscosity values predicted by the DeepModel on the testing set, which consists of droplet images of the formulations PVP07.5, PVP27.5, and PVP42.5 with the measured viscosity values of 1.084, 2.102, and 2.931, respectively, are presented in Figure 7. The figure shows that the majority of the predicted viscosity values are very close to the measured viscosity values of the solution, except for few cases, which may be due to outliers.

The high accuracy the DeepModel achieved on the test set suggests that the model is not only able to learn from the training data but also capture the underlying patterns in the samples that can generalize well to new, similar chemical formulations. Moreover, the accuracy values achieved on both the training and validation sets indicate that the model is not overfitting to the training data but rather effectively generalizing to new data.

Our findings suggest that CNNs offer an advantage in that they can learn and identify patterns in a dataset without prior knowledge of the underlying physical laws governing the behavior of liquids. Specifically, our DeepModel trained on water and PVP solutions can accurately predict the viscosity of liquids with the same composition. However, we

acknowledge that this approach is limited to the specific composition used in the training dataset and cannot be generalized to other types of liquids or polymers.

That being said, we believe that this method has potential applications in scenarios where real-time monitoring of liquid viscosity is required. While we do not propose it as a replacement for traditional viscometers, it can serve as a cost-effective alternative for certain use cases. Additionally, the calibration process is simple and can be completed in a matter of hours with only a few solutions required.

**Table 4.** Results of the different models on the training, validation, and testing sets. The best-performing model is marked with \*.

	SimpleModel	DeepModel *	ComplexModel
Results on the training set			
MSE	0.1297	0.0144	0.0185
MAE	0.3010	0.0906	0.1092
R2	0.8328	0.9813	0.9761
Results on the validation set			
MSE	0.1530	0.0142	0.0223
MAE	0.3215	0.0903	0.1186
R2	0.8174	0.9829	0.9733
Results on the testing set			
MSE	0.1798	0.0243	0.0400
MAE	0.3633	0.0971	0.1504
R2	0.6867	0.9576	0.9302

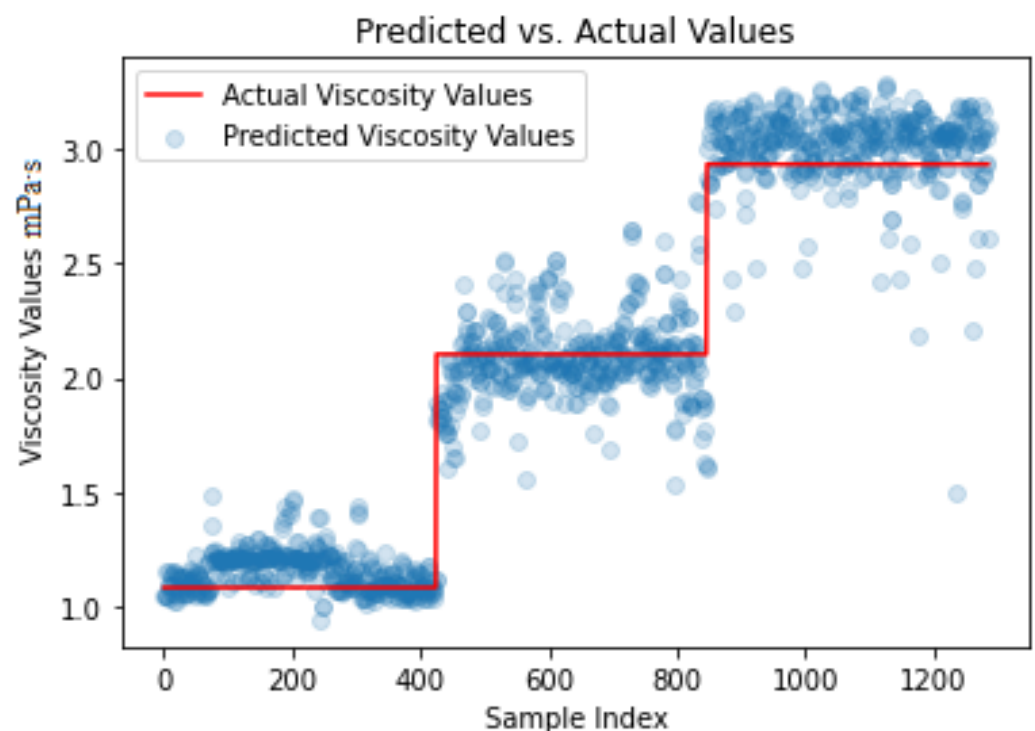


**Figure 7.** Predicted vs. actual viscosity values of DeepModel on testing set.

#### 4. Conclusions

In this study, we have presented a novel approach for estimating the viscosity values of different water–PVP solutions using a convolutional neural network model trained on images of droplets. Our approach is based on the idea that the characteristics of the droplets can provide useful information about their viscosity, and we have demonstrated that a

CNN model can effectively learn this relationship and accurately predict the corresponding viscosity values. Fourteen distinct samples were prepared using different water–PVP ratios, their viscosity values were measured using a viscometer, and their droplets were captured on video using a high-quality monochrome camera. The videos were used to extract images of the droplets just before their detachment. We divided our fourteen chemical formulations into training and testing sets, and we kept all the images from three formulations for testing. We then selected three models with different architectures and evaluated their performance using their mean squared error (MSE), mean absolute error (MAE), and R2 scores. The results indicated that the DeepModel architecture was the most effective, achieving low MSE scores of 0.0144, 0.0142, and 0.0243 on the training, validation, and testing sets, respectively, and R2 scores of 0.9813, 0.9829, and 0.9576 on the same sets, respectively. These values indicate that the model can accurately estimate the viscosity of new, unseen samples of similar chemical formulations, demonstrating its robustness and generalization capability. This method has potential applications in scenarios where real-time monitoring of liquid viscosity is required. It can serve as a cost-effective alternative for certain use cases, especially since its calibration process is simple and can be completed in a matter of hours with only a few solutions required. Specifically, our proposed model trained on water and PVP solutions can accurately estimate the viscosity of liquids with the same composition.

Overall, the results of this study demonstrate the potential of machine learning techniques, particularly CNN models, in solving complex problems in experimental sciences.

**Author Contributions:** Conceptualization, M.A.M.; data curation, M.A.M. and D.L.G.; methodology, M.A.M. and D.L.G.; resources, D.L.G.; software, M.A.M.; supervision, K.C., D.L.G., and Z.K.N.; validation, M.A.M.; visualization, M.A.M.; writing—original draft, M.A.M.; writing—review and editing, M.A.M., K.C. and H.C. All authors have read and agreed to the published version of the manuscript.

**Funding:** Project no. 2019-1.3.1-KK-2019-00004 has been implemented with the support provided from the National Research, Development and Innovation Fund of Hungary, financed under the 2019-1.3.1-KK funding scheme.

**Institutional Review Board Statement:** Not applicable.

**Informed Consent Statement:** Not applicable.

**Data Availability Statement:** Data supporting the reported results can be found on the following github repository: <https://github.com/mradazzouz/ViscosityEstimation/> (accessed on 25 June 2023).

**Conflicts of Interest:** The authors declare no conflict of interest.

## Abbreviations

The following abbreviations are used in this manuscript:

CNN Convolutional Neural Network  
PVP Polyvinylpyrrolidone

## References

1. Viswanath, D.S.; Ghosh, T.K.; Prasad, D.H.; Dutt, N.V.; Rani, K.Y. *Viscosity of Liquids: Theory, Estimation, Experiment, and Data*; Springer Science & Business Media: Dordrecht, The Netherlands, 2007.
2. Toropainen, E.; Fraser-Miller, S.J.; Novakovic, D.; Del Amo, E.M.; Vellonen, K.S.; Ruponen, M.; Viitala, T.; Korhonen, O.; Auriola, S.; Hellinen, L.; et al. Biopharmaceutics of topical ophthalmic suspensions: Importance of viscosity and particle size in ocular absorption of indomethacin. *Pharmaceutics* **2021**, *13*, 452. [[CrossRef](#)] [[PubMed](#)]
3. Lokhande, A.B.; Mishra, S.; Kulkarni, R.D.; Naik, J.B. Influence of different viscosity grade ethylcellulose polymers on encapsulation and in vitro release study of drug loaded nanoparticles. *J. Pharm. Res.* **2013**, *7*, 414–420. [[CrossRef](#)]
4. Bourne, M. *Food Texture and Viscosity: Concept and Measurement*; Elsevier: Amsterdam, The Netherlands, 2002.

5. Nunes, V.M.; Lourenço, M.J.; Santos, F.J.; Nieto de Castro, C.A. Importance of accurate data on viscosity and thermal conductivity in molten salts applications. *J. Chem. Eng. Data* **2003**, *48*, 446–450. [[CrossRef](#)]
6. Rashid, B.; Bal, A.L.; Williams, G.J.; Muggeridge, A.H. Using vorticity to quantify the relative importance of heterogeneity, viscosity ratio, gravity and diffusion on oil recovery. *Comput. Geosci.* **2012**, *16*, 409–422. [[CrossRef](#)]
7. Hemmati-Sarapardeh, A.; Shokrollahi, A.; Tatar, A.; Gharagheizi, F.; Mohammadi, A.H.; Naseri, A. Reservoir oil viscosity determination using a rigorous approach. *Fuel* **2014**, *116*, 39–48. [[CrossRef](#)]
8. Brooks, R.; Dinsdale, A.; Quedsted, P. The measurement of viscosity of alloys—A review of methods, data and models. *Meas. Sci. Technol.* **2005**, *16*, 354. [[CrossRef](#)]
9. Zhao, H.; Memon, A.; Gao, J.; Taylor, S.D.; Sieben, D.; Ratulowski, J.; Alboudwarej, H.; Pappas, J.; Creek, J. Heavy oil viscosity measurements: Best practices and guidelines. *Energy Fuels* **2016**, *30*, 5277–5290. [[CrossRef](#)]
10. Caponi, M.; Cox, A.; Misra, S. Viscosity prediction using image processing and supervised learning. *Fuel* **2023**, *339*, 127320. [[CrossRef](#)]
11. Zhang, T.; Cao, D.; Feng, X.; Zhu, J.; Lu, X.; Mu, L.; Qian, H. Machine learning prediction of bio-oil characteristics quantitatively relating to biomass compositions and pyrolysis conditions. *Fuel* **2022**, *312*, 122812. [[CrossRef](#)]
12. Cengiz, E.; Babagiray, M.; Aysal, F.E.; Aksoy, F. Kinematic viscosity estimation of fuel oil with comparison of machine learning methods. *Fuel* **2022**, *316*, 123422. [[CrossRef](#)]
13. Rahmanifard, H.; Maroufi, P.; Alimohamadi, H.; Plaksina, T.; Gates, I. The application of supervised machine learning techniques for multivariate modelling of gas component viscosity: A comparative study. *Fuel* **2021**, *285*, 119146. [[CrossRef](#)]
14. Afrand, M.; Najafabadi, K.N.; Sina, N.; Safaei, M.R.; Kherbeet, A.S.; Wongwises, S.; Dahari, M. Prediction of dynamic viscosity of a hybrid nano-lubricant by an optimal artificial neural network. *Int. Commun. Heat Mass Transf.* **2016**, *76*, 209–214. [[CrossRef](#)]
15. Esfe, M.H.; Saedodin, S.; Sina, N.; Afrand, M.; Rostami, S. Designing an artificial neural network to predict thermal conductivity and dynamic viscosity of ferromagnetic nanofluid. *Int. Commun. Heat Mass Transf.* **2015**, *68*, 50–57. [[CrossRef](#)]
16. Al-Amoudi, L.A.; Patil, S.; Baarimah, S.O. Development of artificial intelligence models for prediction of crude oil viscosity. In Proceedings of the SPE Middle East Oil and Gas Show and Conference, Manama, Bahrain, 18–21 March 2019; OnePetro: Richardson, TX, USA, 2019.
17. Omole, O.; Falode, O.; Deng, A.D. Prediction of Nigerian crude oil viscosity using artificial neural network. *Pet. Coal* **2009**, *51*, 181–188.
18. Zhu, H.; Dexter, R.; Fox, R.; Reichard, D.; Brazee, R.; Ozkan, H. Effects of polymer composition and viscosity on droplet size of recirculated spray solutions. *J. Agric. Eng. Res.* **1997**, *67*, 35–45. [[CrossRef](#)]
19. Wang, Z.; Liu, H.; Zhang, Z.; Sun, B.; Zhang, J.; Lou, W. Research on the effects of liquid viscosity on droplet size in vertical gas–liquid annular flows. *Chem. Eng. Sci.* **2020**, *220*, 115621. [[CrossRef](#)]
20. Gotaas, C.; Havelka, P.; Jakobsen, H.A.; Svendsen, H.F.; Hase, M.; Roth, N.; Weigand, B. Effect of viscosity on droplet-droplet collision outcome: Experimental study and numerical comparison. *Phys. Fluids* **2007**, *19*, 102106. [[CrossRef](#)]
21. Kheloufi, N.; Lounis, M. An Optical Technique for Newtonian Fluid Viscosity Measurement Using Multiparameter Analysis. *Appl. Rheol.* **2014**, *24*, 15–22.
22. Mrad, M.A.; Csorba, K.; Galata, D.L.; Nagy, Z.K. Classification of Droplets of Water-PVP Solutions with Different Viscosity Values Using Artificial Neural Networks. *Processes* **2022**, *10*, 1780. [[CrossRef](#)]
23. Santhosh, K.; Shenoy, V. Analysis of liquid viscosity by image processing techniques. *Indian J. Sci. Technol.* **2016**, *9*, 98693. [[CrossRef](#)]
24. Sakib, S.; Ahmed, N.; Kabir, A.J.; Ahmed, H. An overview of convolutional neural network: Its architecture and applications. *Preprints.org* **2019**, *in press*.
25. Iwata, H.; Hayashi, Y.; Hasegawa, A.; Terayama, K.; Okuno, Y. Classification of scanning electron microscope images of pharmaceutical excipients using deep convolutional neural networks with transfer learning. *Int. J. Pharm.* **2022**, *4*, 100135. [[CrossRef](#)]
26. Ghorbani, Z.; Behzadan, A.H. Monitoring offshore oil pollution using multi-class convolutional neural networks. *Environ. Pollut.* **2021**, *289*, 117884. [[CrossRef](#)]
27. Vasconcelos, L.; Kijanka, P.; Urban, M.W. Viscoelastic parameter estimation using simulated shear wave motion and convolutional neural networks. *Comput. Biol. Med.* **2021**, *133*, 104382. [[CrossRef](#)]
28. Vishnu Mohan, M.S.; Menon, V. Measuring Viscosity of Fluids: A Deep Learning Approach Using a CNN-RNN Architecture. In Proceedings of the First International Conference on AI-ML-Systems, Bangalore, India, 21–23 October 2021; pp. 1–5.
29. Mineshita, T.; Watanabe, T.; Ono, S. The flow properties of polyvinylpyrrolidone solutions. *Bull. Chem. Soc. Jpn.* **1967**, *40*, 2217–2223. [[CrossRef](#)]
30. Naveenkumar, M.; Vadivel, A. OpenCV for computer vision applications. In Proceedings of the National Conference on Big Data and Cloud Computing (NCBDC'15), Tiruchirappalli, India, 20 March 2015; pp. 52–56.

31. Gu, J.; Wang, Z.; Kuen, J.; Ma, L.; Shahroudy, A.; Shuai, B.; Liu, T.; Wang, X.; Wang, G.; Cai, J.; et al. Recent advances in convolutional neural networks. *Pattern Recognit.* **2018**, *77*, 354–377. [[CrossRef](#)]
32. Manaswi, N.K. Understanding and working with Keras. In *Deep Learning with Applications Using Python*; Springer: New York, NY, USA, 2018; pp. 31–43.

**Disclaimer/Publisher’s Note:** The statements, opinions and data contained in all publications are solely those of the individual author(s) and contributor(s) and not of MDPI and/or the editor(s). MDPI and/or the editor(s) disclaim responsibility for any injury to people or property resulting from any ideas, methods, instructions or products referred to in the content.